

# Graphical CSS Code Transformation Using ZX Calculus

Jiaxin Huang\*

Dept. of Computer Science  
Hong Kong University of  
Science and Technology  
jhuangbo@connect.ust.hk

Sarah Meng Li\*

Institute for Quantum Computing (IQC)  
Dept. of Combinatorics & Optimization (C&O)  
University of Waterloo  
sarah.li@uwaterloo.ca

Lia Yeh\*

University of Oxford  
Quantinuum  
17 Beaumont Street  
Oxford OX1 2NA, UK  
lia.yeh@cs.ox.ac.uk

Aleks Kissinger

University of Oxford  
aleks.kissinger@cs.ox.ac.uk

Michele Mosca

Perimeter Institute (PI)  
IQC, C&O, University of Waterloo  
michele.mosca@uwaterloo.ca

Michael Vasmer

PI, IQC, University of Waterloo  
mvasmer@perimeterinstitute.ca

In this work, we present a generic approach to transform CSS codes by building upon their equivalence to phase-free ZX diagrams. Using the ZX calculus, we demonstrate diagrammatic transformations between encoding maps associated with different codes. As a motivating example, we give explicit transformations between the Steane code and the quantum Reed-Muller code, since by switching between these two codes, one can obtain a fault-tolerant universal gate set. To this end, we propose a bidirectional rewrite rule to find a (not necessarily transversal) physical implementation for any logical ZX diagram in any CSS code.

We then focus on two code transformation techniques: *code morphing*, a procedure that transforms a code while retaining its fault-tolerant gates, and *gauge fixing*, where complimentary codes can be obtained from a common subsystem code (e.g., the Steane and the quantum Reed-Muller codes from the  $[[15, 1, 3, 3]]$  code). We provide explicit graphical derivations for these techniques and show how ZX and graphical encoder maps relate several equivalent perspectives on these code transforming operations.

## 1 Introduction

Quantum computation has demonstrated its potential in speeding up large-scale computational tasks [3, 68] and revolutionizing multidisciplinary fields such as drug discovery [11], climate prediction [60], chemistry simulation [47], and the quantum internet [25]. However, in a quantum system, qubits are sensitive to interference and information becomes degraded [50]. To this end, quantum error correction [55, 57] and fault tolerance [33, 41] have been developed to achieve large-scale universal quantum computation [34].

Stabilizer theory [32] is a mathematical framework to describe and analyze properties of quantum error-correcting codes (QECC). It is based on the concept of stabilizer groups, which are groups of Pauli operators whose joint  $+1$  eigenspace corresponds to the code space. Stabilizer codes are a specific type of QECC whose encoder can be efficiently simulated [1, 31]. As a family of stabilizer codes, Calderbank-Shor-Steane (CSS) codes permit simple code constructions from classical codes [9, 10, 57, 58].

As a language for rigorous diagrammatic reasoning of quantum computation, the ZX calculus consists of ZX diagrams and a set of rewrite rules [16, 66]. It has been used to relate stabilizer theory to graphical normal forms: notably, efficient axiomatization of the stabilizer fragments for qubits [4, 36, 49],

---

\*equal authorship

qutrits [61, 65], and prime-dimensional qudits [8]. This has enabled various applications, such as measurement-based quantum computation [49, 56], quantum circuit optimization [19, 30] and verification [46], as well as classical simulation [14, 40]. Beyond these, ZX-calculus has been applied to verify QECC [23, 26], represent Clifford encoders [38], as well as study various QECC such as tripartite coherent parity check codes [12, 13] and surface codes [27, 28, 29, 54]. Specific to CSS codes, ZX-calculus has been used to visualize their encoders [39], code maps and code surgeries [22], their correspondence to affine Lagrangian relations [20], and their constructions in high-dimensional quantum systems [21].

In this paper, we seek to answer some overarching questions about QECC constructions and fault-tolerant implementations. We focus on CSS codes and leverage the direct correspondence between phase-free ZX diagrams and CSS code encoders [39]. Given an arbitrary CSS code, based on its normal form, we propose a bidirectional rewrite rule to find a (not necessarily transversal) physical implementation for any logical ZX diagram. Furthermore, we demonstrate diagrammatic transformations between encoding maps associated with different codes. Here, we focus on two code transformation techniques: *code morphing*, a procedure that transforms a code while retaining its fault-tolerant gates [62], and *gauge fixing*, where complimentary codes (such as the Steane and the quantum Reed-Muller codes) can be obtained from a common subsystem code [2, 51, 53, 64]. We provide explicit graphical derivations for these techniques and show how ZX and graphical encoder maps relate several equivalent perspectives on these code transforming operations.

The rest of this paper is organized as follows. In Sec. 2, we introduce notions and techniques used to graphically transform different CSS codes using the ZX calculus. In Sec. 3, we generalize the ZX normal form for CSS stabilizer codes to CSS subsystem codes, and provide generic bidirectional rewrite rules for any CSS encoder. In Sec. 4, we provide explicit graphical derivations for morphing the Steane and the quantum Reed-Muller codes. In Sec. 5, we focus on the switching protocol between these two codes. Through ZX calculus, we provide a graphical interpretation of this protocol as gauge-fixing the  $[[15, 1, 3, 3]]$  subsystem code, followed by syndrome-determined recovery operations. We conclude with Sec. 6.

## 2 Preliminaries

We start with some definitions. The Pauli matrices are  $2 \times 2$  unitary operators acting on a single qubit. Let  $i$  be the imaginary unit.

$$I = \begin{bmatrix} 1 & 0 \\ 0 & 1 \end{bmatrix}, \quad X = \begin{bmatrix} 0 & 1 \\ 1 & 0 \end{bmatrix}, \quad Z = \begin{bmatrix} 1 & 0 \\ 0 & -1 \end{bmatrix}, \quad Y = iXZ = \begin{bmatrix} 0 & -i \\ i & 0 \end{bmatrix}.$$

Let  $\mathcal{P}_1$  be the single-qubit Pauli group,  $\mathcal{P}_1 = \langle i, X, Z \rangle$ ,  $I, Y \in \mathcal{P}_1$ .

**Definition 2.1.** Let  $U \in \mathcal{U}(2)$ . In a system over  $n$  qubits,  $1 \leq i \leq n$ ,

$$U_i = I \otimes \dots \otimes I \otimes U \otimes I \otimes \dots \otimes I$$

denotes  $U$  acting on the  $i$ -th qubit, and identity on all other qubits.

Let  $\mathcal{P}_n$  be the  $n$ -qubit Pauli group. It consists of all tensor products of single-qubit Pauli operators.

$$\mathcal{P}_n = \langle i, X_1, Z_1, \dots, X_n, Z_n \rangle.$$

The stabilizer formalism is a mathematical framework to describe and analyze the properties of certain QECC, called stabilizer codes [32, 33]. Consider  $n$  qubits and let  $m \leq n$ . A stabilizer group  $\mathcal{S} = \langle S_1, \dots, S_m \rangle$  is an Abelian subgroup of  $\mathcal{P}_n$  that does not contain  $-I$ . The codespace of the corresponding stabilizer code,  $\mathcal{C}$ , is the joint  $+1$  eigenspace of  $\mathcal{S}$ , i.e.,

$$\mathcal{C} = \{|\psi\rangle \in \mathbb{C}^{2^n}; \mathcal{S}|\psi\rangle = |\psi\rangle, \forall S \in \mathcal{S}\}.$$

The number of encoded qubits in a stabilizer code is  $k = n - m$ , where  $m$  is the number of independent stabilizer generators [32]. Moreover, we can define the *centralizer* of  $\mathcal{S}$  as

$$\mathcal{N}(\mathcal{S}) = \{U \in \mathcal{P}_n; [U, S] = 0, \forall S \in \mathcal{S}\}.$$

One can check that  $\mathcal{N}(\mathcal{S})$  is a subgroup of  $\mathcal{P}_n$  and  $\mathcal{S} \subset \mathcal{N}(\mathcal{S})$ . We remark that the notions of normalizer and centralizer coincide for any stabilizer group. In what follows, we will use them interchangeably. As we will see later,  $\mathcal{N}(\mathcal{S})$  provides an algebraic structure for the subsystem codes. The code distance,  $d$ , of a stabilizer code is the minimal weight of operators in  $\mathcal{N}(\mathcal{S})/\langle iI \rangle$  that is not in  $\mathcal{S}$ . We summarize the properties of a stabilizer code with the shorthand  $\llbracket n, k, d \rrbracket$ .

Finally, we introduce some notation for subsets of  $n$ -qubit Pauli operators, which will prove useful for defining CSS codes.

**Definition 2.2.** Let  $M$  be an  $m \times n$  binary matrix and  $P \in \mathcal{P}_1/\langle iI \rangle$ . In the stabilizer formalism,  $M$  is called the stabilizer matrix, and  $M^P$  defines  $m$   $P$ -type stabilizer generators.

$$M^P := \left\{ \bigotimes_{j=1}^n P^{[M]_{ij}}; 1 \leq i \leq m \right\}.$$

CSS codes are QECC whose stabilizers are defined by two orthogonal binary matrices  $G$  and  $H$  [9, 57]:

$$\mathcal{S} = \langle G^X, H^Z \rangle, \quad GH^T = \mathbf{0},$$

$H^T$  is the transpose of  $H$ . This means that the stabilizer generators of a CSS code can be divided into two types: X-type and Z-type. For example, the  $\llbracket 7, 1, 3 \rrbracket$  Steane code [57] in Fig. 1a is specified by

$$G = H = \begin{bmatrix} 1 & 0 & 1 & 0 & 1 & 0 & 1 \\ 0 & 1 & 1 & 0 & 0 & 1 & 1 \\ 0 & 0 & 0 & 1 & 1 & 1 & 1 \end{bmatrix}_{3 \times 7}. \quad (1)$$

Accordingly, the X-type and Z-type stabilizers are defined as

$$S_1^X = X_1 X_3 X_5 X_7, \quad S_2^X = X_2 X_3 X_6 X_7, \quad S_3^X = X_4 X_5 X_6 X_7, \quad S_1^Z = Z_1 Z_3 Z_5 Z_7, \quad S_2^Z = Z_2 Z_3 Z_6 Z_7, \quad S_3^Z = Z_4 Z_5 Z_6 Z_7.$$

The logical operators  $\bar{X}$  and  $\bar{Z}$  are defined as

$$\bar{X} = X_1 X_4 X_5 \quad \text{and} \quad \bar{Z} = Z_1 Z_4 Z_5. \quad (2)$$

In Sec. 2.1, we define CSS subsystem codes. In Sec. 2.2, we define several CSS codes that will be used in subsequent sections. In Sec. 2.3, we introduce the basics of the ZX calculus and the phase-free ZX normal forms.

## 2.1 CSS Subsystem Codes

Subsystem codes [43, 52] are QECC where some of the logical qubits are not used for information storage and processing. These logical qubits are called gauge qubits. By fixing gauge qubits to some specific states, the same subsystem code may exhibit different properties, for instance, having different sets of transversal gates [7, 44, 45, 51, 67]. This provides a tool to circumvent restrictions on transversal gates such as the Eastin-Knill theorem [24].

Based on the construction proposed in [52], we describe a subsystem code using the stabilizer formalism.

**Definition 2.3.** *Given a stabilizer group  $\mathcal{S}$ , a gauge group  $\mathcal{G}$  is a normal subgroup of  $\mathcal{N}(\mathcal{S})$ , such that  $\mathcal{S} \subset \mathcal{G}$  and that  $\mathcal{G}/\mathcal{S}$  contains anticommuting Pauli pairs. In other words, one can write*

$$\mathcal{S} = \langle S_1, \dots, S_m \rangle, \quad \mathcal{G} = \langle S_1, \dots, S_m, g_1^X, g_1^Z, \dots, g_r^X, g_r^Z \rangle, \quad 1 \leq m + r \leq n.$$

$(\mathcal{S}, \mathcal{G})$  defines an  $[[n, k, r, d]]$  subsystem code where  $n = m + k + r$ . The logical operators are elements of the quotient group  $\mathcal{L} = \mathcal{N}(\mathcal{S})/\mathcal{G}$ .

Under this construction,  $n$  physical qubits are used to encode  $k$  logical qubits with  $r$  gauge qubits. Alternatively, we can think of the gauge group  $\mathcal{G}$  as partitioning the code space  $\mathcal{C}$  into two subsystems:  $\mathcal{C} = \mathcal{A} \otimes \mathcal{B}$ . Logical information is encoded in  $\mathcal{A}$  and  $\mathcal{L}$  serves as the group of logical operations. Gauge operators from  $\mathcal{G}$  act trivially on subsystem  $\mathcal{A}$ , while operators from  $\mathcal{L}$  act trivially on subsystem  $\mathcal{B}$ . Therefore, two states  $\rho^{\mathcal{A}} \otimes \rho^{\mathcal{B}}$  and  $\rho'^{\mathcal{A}} \otimes \rho'^{\mathcal{B}}$  are considered equivalent if  $\rho^{\mathcal{A}} = \rho'^{\mathcal{A}}$ , regardless of the states  $\rho^{\mathcal{B}}$  and  $\rho'^{\mathcal{B}}$ . When  $r = 0$ ,  $\mathcal{G} = \mathcal{S}$ . In that case, an  $[[n, k, 0, d]]$  subsystem code is essentially an  $[[n, k, d]]$  stabilizer code.

CSS subsystem codes are subsystem codes whose stabilizer generators can be divided into X-type and Z-type operators. In what follows, we provide an example to illustrate their construction.

## 2.2 Some Interesting CSS Codes

We start by defining the stabilizer groups for the  $[[7, 1, 3]]$  Steane code, the  $[[15, 1, 3]]$  extended Steane code [2], and the  $[[15, 1, 3]]$  quantum Reed-Muller code [42]. They are derived from the family of  $[[2^m - 1, 1, 3]]$  quantum Reed-Muller codes, with a recursive construction of stabilizer matrices [59]. The Steane code has transversal logical Clifford operators, and the quantum Reed-Muller code has a transversal logical T gate. Together these operators form a universal set of fault-tolerant gates. In Sec. 5, the relations between these codes are studied from a diagrammatic perspective.

For brevity, their corresponding stabilizer groups are denoted as  $\mathcal{S}_{steane}$ ,  $\mathcal{S}_{ex}$ , and  $\mathcal{S}_{qrm}$ . As per Def. 2.2, consider three stabilizer matrices  $F$ ,  $H$ , and  $J$ . Note that  $G$  is defined in Eq. (1).  $\mathbf{0}$  and  $\mathbf{1}$  denote blocks of 0s' and 1s' respectively. Their dimensions can be inferred from the context.

$$F = \begin{bmatrix} G & \mathbf{0} & G \\ \mathbf{0} & \mathbf{1} & \mathbf{1} \end{bmatrix}_{4 \times 15}, \quad H = [G \quad \mathbf{0}]_{3 \times 15},$$

$$J = \begin{bmatrix} 1 & 0 & 1 & 0 & 0 & 0 & 0 & 0 & 1 & 0 & 1 & 0 & 0 & 0 & 0 \\ 0 & 1 & 1 & 0 & 0 & 0 & 0 & 0 & 0 & 1 & 1 & 0 & 0 & 0 & 0 \\ 0 & 0 & 1 & 0 & 0 & 0 & 1 & 0 & 0 & 0 & 1 & 0 & 0 & 0 & 1 \end{bmatrix}_{3 \times 15}.$$

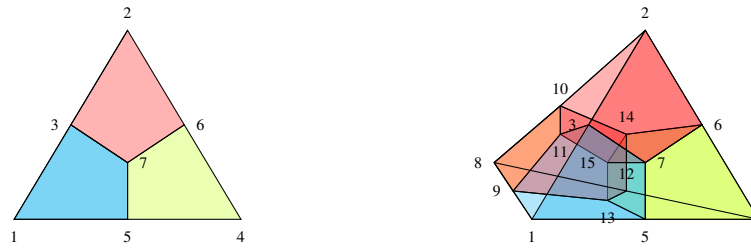
Then, the stabilizer groups are defined as

$$\mathcal{S}_{steane} = \langle G^X, G^Z \rangle, \quad \mathcal{S}_{ex} = \langle F^X, F^Z, H^X, H^Z \rangle, \quad \mathcal{S}_{qrm} = \langle F^X, F^Z, H^Z, J^Z \rangle. \quad (3)$$

Geometrically, one can define  $\mathcal{S}_{steane}$  and  $\mathcal{S}_{qrm}$  with the aid of Fig. 1. In Fig. 1a, the Steane code is visualized on a 2D lattice. Since the Steane code is self-dual, every coloured face corresponds to an X-type and Z-type stabilizer. In Fig. 1b, the quantum Reed-Muller code is visualized on a 3D lattice. Every coloured face corresponds to a weight-4 Z-type stabilizer. Every coloured cell corresponds to a weight-8 X-type stabilizer. For the Steane code, the logical operators defined in Eq. (2) correspond to an edge in the triangle. For the quantum Reed-Muller code, the logical X operator corresponds to a weight-7 triangular face, and the logical Z operator corresponds to a weight-3 edge of the entire tetrahedron. An example is shown below.

$$\bar{X} = X_1X_2X_3X_4X_5X_6X_7 \quad \text{and} \quad \bar{Z} = Z_1Z_4Z_5 \quad (4)$$

Given such representations, the Steane code and the quantum Reed-Muller code are also special cases of colour codes [5, 6, 44].



(a) The Steane code as a 2D colour code. (b) The quantum Reed-Muller as a 3D colour code.

Figure 1: Each vertex represents a physical qubit. Each edge serves as an aid to the eye. They do not imply any physical interactions or inherent structures.

From Eq. (3), the extended Steane code is self-dual, and its encoded state is characterized by the lemma below. It shows that  $\mathcal{S}_{ex}$  and  $\mathcal{S}_{steane}$  are equivalent up to some auxiliary state.

**Lemma 2.1** ([2]). *Any codeword  $|\psi\rangle$  of the extended Steane code can be decomposed into a codeword  $|\phi\rangle$  of the Steane code and a fixed state  $|\eta\rangle$ . That is,*

$$|\psi\rangle = |\phi\rangle \otimes |\eta\rangle,$$

where  $|\eta\rangle = \frac{1}{\sqrt{2}}(|0\rangle|\bar{0}\rangle + |1\rangle|\bar{1}\rangle)$ ,  $|\bar{0}\rangle$  and  $|\bar{1}\rangle$  are the logical 0 and 1 encoded in the Steane code.

Since the logical information  $|\phi\rangle$  encoded in the Steane code is not entangled with  $|\eta\rangle$ , to switch between the Steane code and the extended Steane code, one may simply add or discard the auxiliary state  $|\eta\rangle$ . This property will prove useful in Sec. 5.

Next, we define the  $[[15, 1, 3, 3]]$  CSS subsystem code [64]. As per Def. 2.3, let  $\mathcal{S}_{sub}$  and  $\mathcal{G}$  be its stabilizer group and gauge group respectively.

$$\mathcal{S}_{sub} = \langle F^X, F^Z, H^Z \rangle, \quad \mathcal{G} = \langle F^X, F^Z, H^X, H^Z, J^Z \rangle. \quad (5)$$

Let  $\mathcal{L}_g = \mathcal{G}/\mathcal{S}$  and  $\mathcal{L} = \mathcal{N}(\mathcal{S})/\mathcal{G}$ . One can verify that

$$\mathcal{L}_g = \langle H^X, J^Z \rangle, \quad \mathcal{L} = \langle \bar{X}, \bar{Z} \rangle. \quad (6)$$

Thus, the CSS subsystem code has one logical qubit and three gauge qubits, and they are acted on by  $\mathcal{L}_g$  and  $\mathcal{L}$  respectively. From Sec. 3 onwards, we call operators in  $\mathcal{L}_g$  as *gauge operators*.

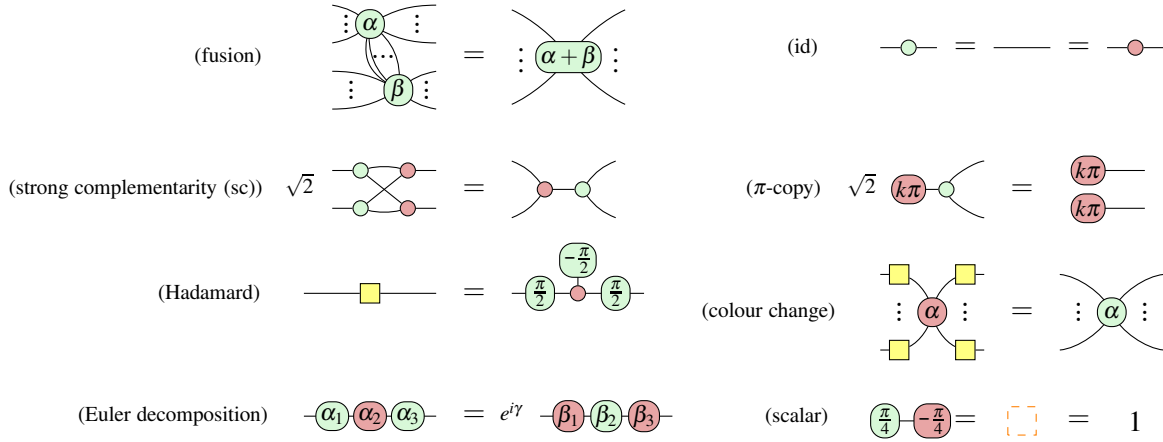


Figure 2: These eight equations suffice to derive all other equalities of linear maps on qubits [63].  $k \in \mathbb{Z}_2$ .  $\alpha_i$ ,  $\beta_i$  and  $\gamma$  are real numbers satisfying the trigonometric relations derived in [18]. Each equation still holds when we replace all spiders with their corresponding spiders of the opposite colour. Whenever there are any two wires with ... between them, the rule holds when replacing this with any number of wires (i.e., 0 or greater).

Moreover,  $\mathcal{S}_{sub}$  can be viewed as the stabilizer group of a  $[[15, 4, 3]]$  CSS code, with logical operators  $\mathcal{L}'$ . This code appears in an intermediary step of the gauge fixing process in Sec. 5.

$$\mathcal{L}' := \mathcal{L}_g \cup \mathcal{L} = \langle H^X, J^Z, \bar{X}, \bar{Z} \rangle. \quad (7)$$

### 2.3 ZX Calculus

The qubit ZX-calculus [15, 16, 17, 66] is a quantum graphical calculus for diagrammatic reasoning of any qubit quantum computation. Every diagram in the calculus is composed of two types of generators: Z spiders, which sum over the eigenbasis of the Pauli Z operator:

$${}_m \langle \text{Z spider with phase } \alpha \rangle_n := |0\rangle^{\otimes n} \langle 0|^{\otimes m} + e^{i\alpha} |1\rangle^{\otimes n} \langle 1|^{\otimes m}, \quad (8)$$

and X spiders, which sum over the eigenbasis of the Pauli X operator:

$${}_m \langle \text{X spider with phase } \alpha \rangle_n := |+\rangle^{\otimes n} \langle +|^{\otimes m} + e^{i\alpha} |-\rangle^{\otimes n} \langle -|^{\otimes m}. \quad (9)$$

The ZX-calculus is *universal* [16] in the sense that any linear map from  $m$  qubits to  $n$  qubits corresponds exactly to a ZX diagram, by the construction of Eqs. (8) and (9) and the composition of linear maps.

Furthermore, the ZX-calculus is *complete* [35, 37]: Any equality of linear maps on any number of qubits derivable in the Hilbert space formalism, is derivable using only a finite set of rules in the calculus. The smallest complete rule set to date [63] is shown in Fig. 2. Some additional rules, despite being derivable from this rule set, will be convenient to use in this paper. They are summarized in Fig. 3.

When a spider has phase zero, we omit its phase in the diagram, as shown below. A ZX diagram is *phase-free* if all of its spiders have zero phases. For more discussions on phase-free ZX diagrams, we refer readers to consult [39].

$$\begin{array}{c} \text{Z spider} \\ \text{with phase } \alpha \end{array} := \begin{array}{c} \text{Z spider} \\ \text{with phase } 0 \end{array} \quad \begin{array}{c} \text{X spider} \\ \text{with phase } \alpha \end{array} := \begin{array}{c} \text{X spider} \\ \text{with phase } 0 \end{array}$$

Due to the universality of the ZX calculus, quantum error-correcting code encoders, as linear isometries, can be drawn as ZX diagrams [38]. Moreover, the encoder for a CSS code corresponds exactly to the phase-free ZX (and XZ) normal form [39].

**Definition 2.4.** For a CSS stabilizer code defined by  $\mathcal{S}$ , let  $\{S_i^x; 1 \leq i \leq m\} \subset \mathcal{S}$  be the X-type stabilizer generators and  $\{\bar{X}_j; 1 \leq j \leq k\}$  be the logical X operators,  $m + k < n$ . Its ZX normal form can be found via the following steps:

- (a) For each physical qubit, introduce an X spider.
- (b) For each X-type stabilizer generator  $S_i^x$  and logical operator  $\bar{X}_j$ , introduce a Z spider and connect it to all X spiders where this operator has support.
- (c) Give each X spider an output wire.
- (d) For each Z spider representing  $\bar{X}_j$ , give it an input wire.

As an example, the ZX normal form for the Steane code is drawn in Fig. 4. The XZ normal form can be constructed based on Z-type stabilizer generators and logical Z operators by inverting the roles of X and Z spiders in the above procedure. In [39], Kissinger gave an algorithm to rewrite any phase-free ZX code diagram into both the ZX and XZ normal forms, and pointed out that it is sufficient to represent a CSS code encoder using either one of the forms.

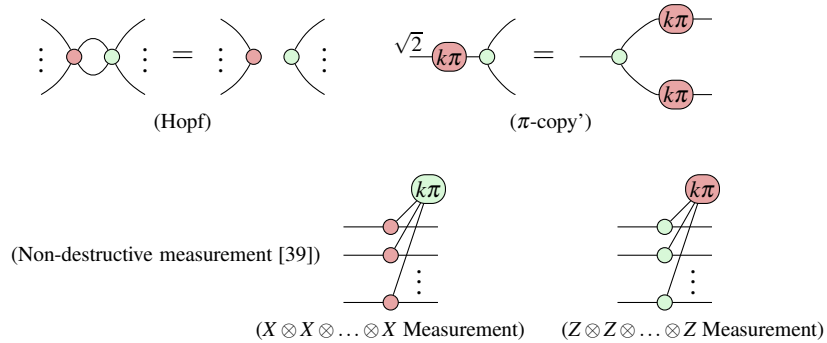


Figure 3: Some other useful rewrite rules, each derivable from the rules in Figure 2.  $k \in \mathbb{Z}_2$ . Each equation still holds when we interchange X and Z spiders.

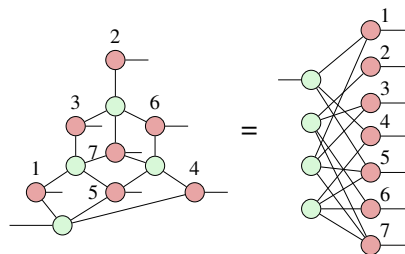


Figure 4: The Steane code encoder in the ZX normal form.

### 3 Graphical Construction of CSS Encoders

#### 3.1 ZX Normal Forms for CSS Subsystem Codes

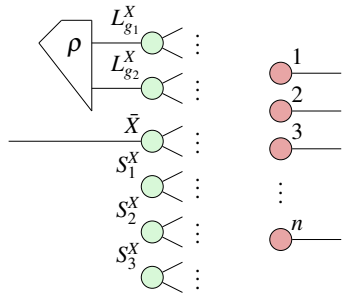
We generalize the ZX normal form for CSS stabilizer codes to CSS subsystem codes as follows.

**Definition 3.1.** For an  $[[n, k, r, d]]$  CSS subsystem code defined by  $(\mathcal{S}, \mathcal{G})$ , let  $\{S_i^x; 1 \leq i \leq m\}$  be the X-type stabilizer generators,  $\{L_{g_t}^x; 1 \leq t \leq r\}$  be the X-type gauge operators, and  $\{\bar{X}_j; 1 \leq j \leq k\}$  be the logical X operators,  $m + k + r < n$ . Its ZX normal form can be found via the following steps:

- For each physical qubit, introduce an X spider.
- For each stabilizer generator  $S_i^x$ , logical operator  $\bar{X}_j$  and gauge operator  $L_{g_t}^x$ , introduce a Z spider and connect it to all X spiders where this operator has support.
- Give each X spider an output wire.
- For each Z spider representing  $\bar{X}_j$ , give it an input wire.
- For all Z spiders representing  $L_{g_t}^x$ , attach to them a joint arbitrary input state (i.e., a density operator  $\rho$ ).

Similar to CSS stabilizer codes, CSS subsystem codes also have an equivalent XZ normal form, which can be found by inverting the role of Z and X in the above procedure.

For  $n > 3$ , below we exemplify the ZX normal form for an  $[[n, 1, 2, d]]$  CSS subsystem code with three X-type stabilizers generators  $\{S_1^x, S_2^x, S_3^x\}$ , two X-type gauge operators  $\{L_{g_1}^x, L_{g_2}^x\}$ , and one logical operator  $\{\bar{X}\}$ . For simplicity, we substitute wires connecting Z and X spiders by  $\frown \therefore$ . The detailed connectivities are omitted here, but they should be clear following step (b) in Def. 3.1. This notation will be used in the remainder of this paper.



### 3.2 Pushing through the Encoder

For any  $[[n, k, d]]$  CSS code, its encoder map  $E$  is of the form:

$$k \left\{ \begin{array}{c} \vdots \\ \vdots \\ \vdots \end{array} \right\} \boxed{E} \left. \begin{array}{c} \vdots \\ \vdots \\ \vdots \end{array} \right\} n.$$

**Definition 3.2.** Let  $\bar{X}_i$  and  $\bar{Z}_i$  be the X and Z operators acting on the  $i$ -th logical qubit. Let  $\bar{\mathcal{X}}_i$  and  $\bar{\mathcal{Z}}_i$  be the physical implementation of  $\bar{X}_i$  and  $\bar{Z}_i$  respectively. Diagrammatically, they can be represented as

$$\begin{array}{c} \vdots \\ \vdots \\ \vdots \end{array} \boxed{\bar{X}_1} \begin{array}{c} \vdots \\ \vdots \\ \vdots \end{array} \boxed{E} \begin{array}{c} \vdots \\ \vdots \\ \vdots \end{array} = \begin{array}{c} \vdots \\ \vdots \\ \vdots \end{array} \boxed{E} \begin{array}{c} \vdots \\ \vdots \\ \vdots \end{array} \boxed{\bar{\mathcal{X}}_1} \begin{array}{c} \vdots \\ \vdots \\ \vdots \end{array} \quad \text{and} \quad \begin{array}{c} \vdots \\ \vdots \\ \vdots \end{array} \boxed{\bar{Z}_1} \begin{array}{c} \vdots \\ \vdots \\ \vdots \end{array} \boxed{E} \begin{array}{c} \vdots \\ \vdots \\ \vdots \end{array} = \begin{array}{c} \vdots \\ \vdots \\ \vdots \end{array} \boxed{E} \begin{array}{c} \vdots \\ \vdots \\ \vdots \end{array} \boxed{\bar{\mathcal{Z}}_1} \begin{array}{c} \vdots \\ \vdots \\ \vdots \end{array} .$$

In other words, pushing  $\bar{X}_i$  (or  $\bar{Z}_i$ ) through  $E$  yields  $\bar{\mathcal{X}}_i$  (or  $\bar{\mathcal{Z}}_i$ ). Using ZX rewrite rules along with the ZX (or XZ) normal form, we can prove the following lemma.

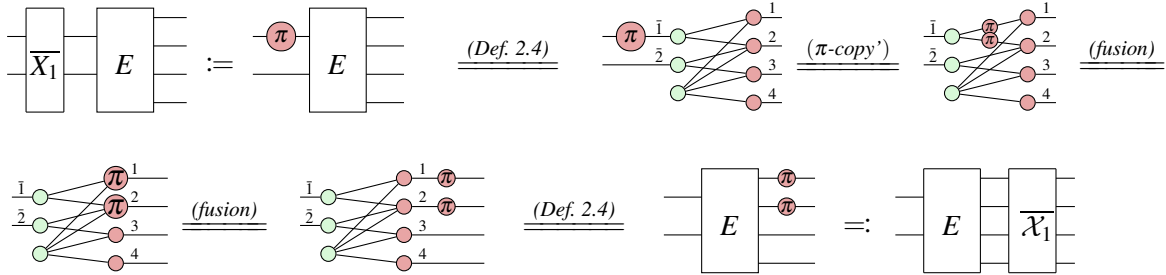


**Lemma 3.1.** For any CSS code, all  $\overline{X}_i$  and  $\overline{Z}_i$  are implementable by multiple single-qubit Pauli operators. In other words, all CSS codes have transversal  $\overline{X}_i$  and  $\overline{Z}_i$ .

*Proof.* Consider an arbitrary CSS code. Without loss of generality, represent its encoder  $E$  in the ZX normal form following Def. 2.4. Then proceed by applying the  $\pi$ -copy' rule on every  $\overline{X}_i$  (the X spider with a phase  $\pi$  on the left-hand side of the encoder  $E$ ).  $\square$

Below we illustrate the proof using the  $[[4, 2, 2]]$  code as an example.

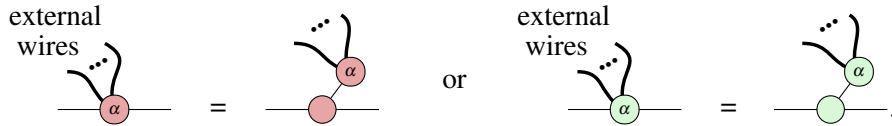
**Example 3.1.** For the  $[[4, 2, 2]]$  code,  $\overline{X}_1 = X_1 X_2$ .



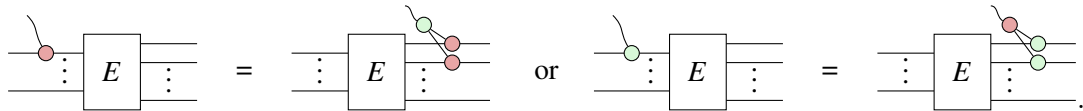
Beyond just X or Z spiders, one can push *any* ZX diagram acting on the logical qubits through the encoder. Such pushing is bidirectional, and the left-to-right direction is interpreted as finding a physical implementation for a given logical operator.

**Proposition 3.1.** Let  $E$  be the encoder of a CSS code. For any ZX diagram  $L$  on the left-hand side of  $E$ , one can write down a corresponding ZX diagram  $P$  on the right-hand side of  $E$ , such that  $EL = PE$ . In other words,  $P$  is a valid physical implementation of  $L$  for that CSS code.

*Proof.* We proceed as follows. First, unfuse all spiders on the logical qubit wires of  $L$ , whenever they are not phase-free or have more than one external wire:



For each X (or Z) spider on the logical qubit wire, rewriting  $E$  to be in ZX (or XZ) normal form and applying the strong complementarity (sc) rule yields:



On the left-hand side, a phase-free X (or Z) spider acts on the  $i$ -th logical qubit; on the right-hand side, phase-free X (or Z) spiders act on all physical qubits wherever  $\overline{X}_i$  (or  $\overline{Z}_i$ ) has support. Therefore, any type of  $L$  can be pushed through  $E$ , resulting in a diagram  $P$  which satisfies  $EL = PE$ .  $\square$

In [26], it was proved that a physical implementation  $P$  of a logical operator  $L$  satisfies  $L = E^\dagger P E$ . This is implied by  $EL = PE$  as  $E^\dagger E = I$ .

## 4 Graphical Morphing of CSS Codes

One way to transform CSS codes is known as *code morphing*. It provides a systematic framework to construct new codes from an existing code while preserving the number of logical qubits in the morphed code. Here, we present this procedure through the rewrites of the encoder diagram using the ZX calculus. Let us start by revisiting the code morphing definition in [62].

**Definition 4.1.** Let  $S$  be a stabilizer group and  $\mathcal{C}$  be its joint  $+1$  eigenspace.  $\mathcal{C}$  is called the parent code. Let  $Q$  denote the set of physical qubits of  $\mathcal{C}$  and  $R \subseteq Q$ . Then  $S(R)$  is a subgroup of  $S$  generated by all stabilizers of  $S$  that are fully supported on  $R$ . Let  $\mathcal{C}(R)$  be the joint  $+1$  eigenspace of  $S(R)$ , and  $\mathcal{C}(R)$  is called the child code. Given the parent code encoder  $E_{\mathcal{C}}$ , concatenate it with the inverse of the child code encoder  $E_{\mathcal{C}(R)}^\dagger$ . This gives the morphed code  $\mathcal{C}_{\setminus R}$ .

Fig. 5 provides two equivalent interpretations for the code morphing process. In Fig. 5a, Def. 4.1 is depicted by the circuit diagram. Since  $E_{\mathcal{C}(R)}$  is an isometry,  $E_{\mathcal{C}(R)}^\dagger E_{\mathcal{C}(R)} = I$ . By construction, the equation shown in Fig. 5a holds [62]. Moreover, the parameters of  $\mathcal{C} = \llbracket n, k, d \rrbracket$ ,  $\mathcal{C}(R) = \llbracket n_1, k_1, d_1 \rrbracket$ , and  $\mathcal{C}_{\setminus R} = \llbracket n_2, k_2, d_2 \rrbracket$  are characterized below. Let  $m, m_1, m_2$  be the number of stabilizer generators for  $\mathcal{C}$ ,  $\mathcal{C}(R)$ , and  $\mathcal{C}_{\setminus R}$  respectively. Then

$$n_2 = n - n_1 + k_1, \quad k_2 = k, \quad m_2 = (n - k) - (n_1 - k_1) = m - m_1, \quad d_1, d_2 \in \mathbb{N}.$$

Fig. 5b provides a concrete example of applying Def. 4.1 to the  $\llbracket 7, 1, 3 \rrbracket$  Steane code, where  $S = \{1, 2, 3, 4, 5, 6, 7\}$  and  $R = \{2, 3, 6, 7\}$ . As a result, the  $\llbracket 5, 1, 2 \rrbracket$  code is morphed from the parent code along with the  $\llbracket 4, 2, 2 \rrbracket$  child code. This morphed code inherits a fault-tolerant implementation of the Clifford group from the  $\llbracket 7, 1, 3 \rrbracket$  code, which has a transversal implementation of the logical Clifford operators. This morphing process is represented in the ZX diagram by cutting the edges labelled by  $\bar{1}$  and  $\bar{2}$  adjacent to the X spider. This is equivalent to concatenating the ZX diagram of  $E_{\llbracket 4, 2, 2 \rrbracket}^\dagger$  in Fig. 5a.

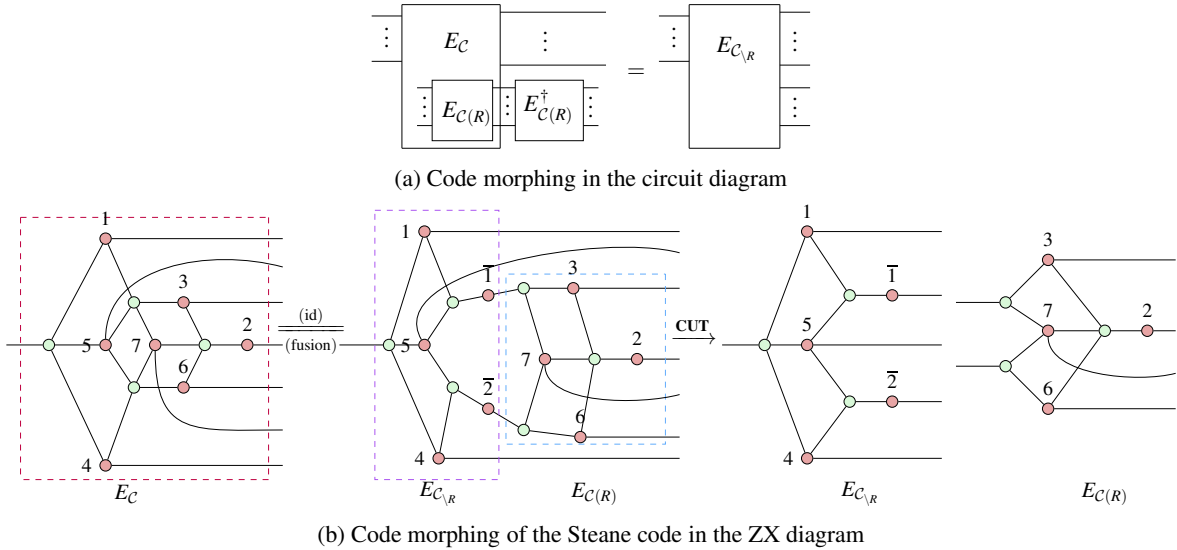


Figure 5: Code morphing can be visualized using both circuit and ZX diagrams. In Fig. 5a, code morphing is viewed as a concatenation of the parent code encoder  $E_{\mathcal{C}}$  and the inverse of the child code encoder  $E_{\mathcal{C}(R)}^\dagger$ . In Fig. 5b, the encoder  $E_{\mathcal{C}}$  of the Steane code is represented in the ZX normal form. As described in Proc. 4.1, by applying ZX rules (id) and (fusion) in Fig. 2, we can perform code morphing by bipartitioning it into the encoder  $E_{\mathcal{C}_{\setminus R}}$  of the morphed code  $\mathcal{C}_{\setminus R} = \llbracket 5, 1, 2 \rrbracket$ , and the encoder  $E_{\mathcal{C}(R)}$  of the child code  $\mathcal{C}(R) = \llbracket 4, 2, 2 \rrbracket$ .

Next, we generalize the notion of code morphing and show how ZX calculus could be used to study these relations between the encoders of different CSS codes. More precisely, we provide an algorithm to morph a new CSS code from an existing CSS code.

**Procedure 4.1.** *Given a parent code  $C$  and a child code  $C(R)$  satisfying Def. 4.1, construct the encoder of  $C$  in the ZX normal form. Then the code morphing proceeds as follows:*

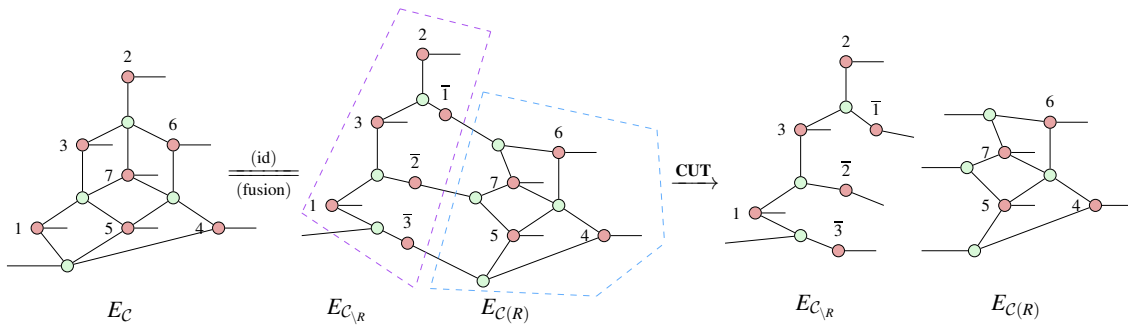
- (a) *Unfuse every Z spider which is supported on  $c$  qubits within  $R$  and  $f$  qubits outside  $R$ ,  $c \neq 0$ ,  $f \neq 0$ .*
- (b) *Add an identity X spider between each pair of Z spiders being unfused in step (a).*
- (c) *Cut the edge between every identity X spider and the Z spiders supported on the  $f$  qubits in  $R$ .*

It follows that the subdiagram containing  $R$  corresponds to the ZX normal form of  $E_{C(R)}$ . It has the same number of X spiders as  $R$ , so  $n_1 = |R|$ . Suppose that there are  $h$  Z spiders being unfused. Then  $h$  must be bounded by the number of Z spiders in the ZX normal form of  $E_C$ . As each spider unfusion introduces a logical qubit to  $C(R)$ ,  $k_1 = h$ . On the other hand, the complement subdiagram contains  $n - n_1 + k_1$  X spiders as each edge cut introduces a new X spider into the complement subdiagram. It also contains  $k$  logical qubits as the input edges in the ZX normal form of  $E_C$  are invariant throughout the spider-unfusing and edge-cutting process. This gives the ZX normal form for the encoder of the morphed code  $C_{\setminus R} = \llbracket n_2, k_2, d_2 \rrbracket$ , where  $n_2 = n - n_1 + k_1$ ,  $k_2 = k$ ,  $d_2 \in \mathbb{N}$ . As a result, the ZX normal form of  $E_C$  is decomposed into the ZX normal forms of  $E_{C(R)}$  and  $E_{C_{\setminus R}}$  respectively.

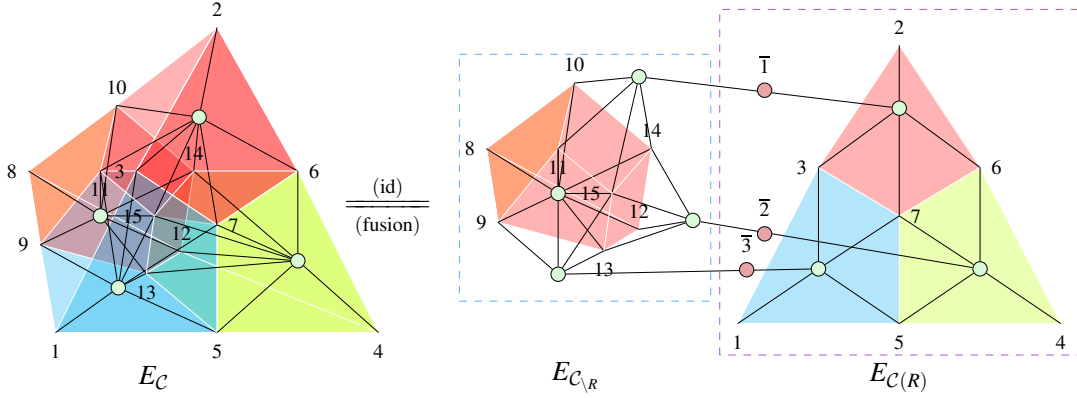
As the XZ and ZX normal forms are equivalent for CSS codes, Proc. 4.1 can be carried out for the XZ normal form by inverting the roles of Z and X at each step.

Here, we exemplify the application of Proc. 4.1 by morphing two simple CSS codes. Unlike Fig. 5b, Ex. 4.1 chooses a different subset of qubits,  $R = \{4, 5, 6, 7\}$ , to obtain the  $\llbracket 6, 1, 1 \rrbracket$  morphed code. In Ex. 4.2, we visualize the  $\llbracket 10, 1, 2 \rrbracket$  code morphing from the  $\llbracket 15, 1, 3 \rrbracket$  quantum Reed-Muller code. The  $\llbracket 10, 1, 2 \rrbracket$  code is interesting because it inherits a fault-tolerant implementation of the logical  $T$  gate from its parent code, which has a transversal implementation of the logical  $T$  gate.

**Example 4.1.** *Let the parent code  $C$  be the Steane code and the child code be  $C(R) = \llbracket 4, 3, 1 \rrbracket$ . By Proc. 4.1, we obtain the morphed code  $C_{\setminus R} = \llbracket 6, 1, 1 \rrbracket$ . Note that for  $C(R)$ , there is one X-type stabilizer generator and no Z-type stabilizer generator. This means that  $C(R)$  cannot detect a single-qubit X error, so it has a distance of 1. In  $C_{\setminus R}$ , the physical qubit labelled  $\bar{3}$  is not protected by any X-type stabilizer. Therefore,  $C_{\setminus R}$  is of distance 1.*



**Example 4.2.** *Let the parent code  $C$  be the quantum Reed-Muller and the child code be  $C(R) = \llbracket 8, 3, 2 \rrbracket$ . By Proc. 4.1, we obtain the morphed code  $C_{\setminus R} = \llbracket 10, 1, 2 \rrbracket$ . For brevity, the X spiders representing physical qubits and the logical qubit wires inputting to the Z spiders are omitted.*



## 5 Graphical Code Switching of CSS Codes

Another way to transform CSS codes is known as *code switching*. It is a widely studied technique in quantum error correction. Codes with complementary fault-tolerant gate sets are switched between each other to realize a universal set of logical operations. As a case study, we focus on the code switching protocol between the Steane code and the quantum Reed-Muller code [2, 51, 53]. Since this process is bidirectional, the reasoning for one direction can be simply adjusted for the opposite direction. Recall in Lem. 2.1, we showed that the extended Steane code is equivalent to the Steane code up to some auxiliary state. In what follows, we focus on the *backward switching* from the quantum Reed-Muller code to the extended Steane code.

Using the ZX calculus, we provide a graphical interpretation for the backward code switching. More precisely, it is visualized as gauge-fixing the  $[[15, 1, 3, 3]]$  subsystem code, followed by a sequence of syndrome-determined recovery operations.

We first characterize the relations between the quantum Reed-Muller code, the extended Steane code, and the  $[[15, 1, 3, 3]]$  subsystem code. For brevity, we denote these codes as  $C_{qrm}$ ,  $C_{ex}$  and  $C_{sub}$ , and their respective encoders as  $E_{qrm}$ ,  $E_{ex}$ , and  $E_{sub}$ .

**Lemma 5.1.** *When the three gauge qubits are in the  $|+++ \rangle$  state,  $C_{sub}$  is equal to  $C_{ex}$ , as shown in Fig. 6.*

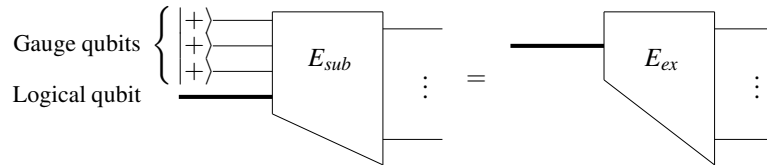
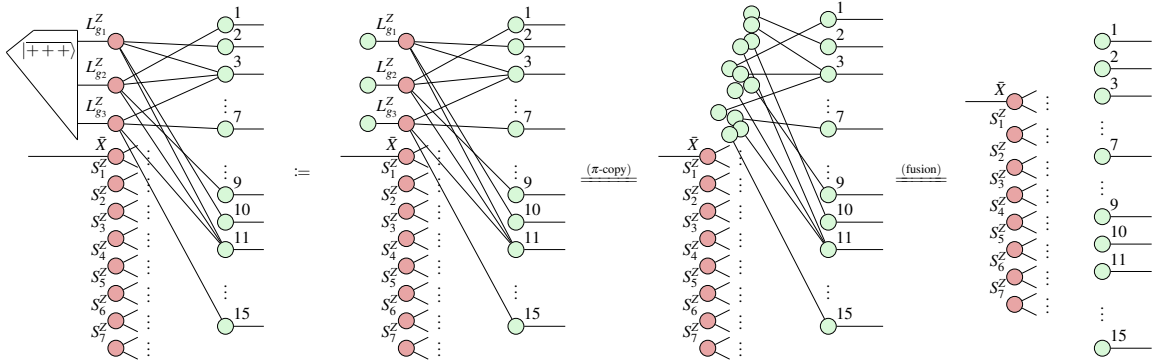


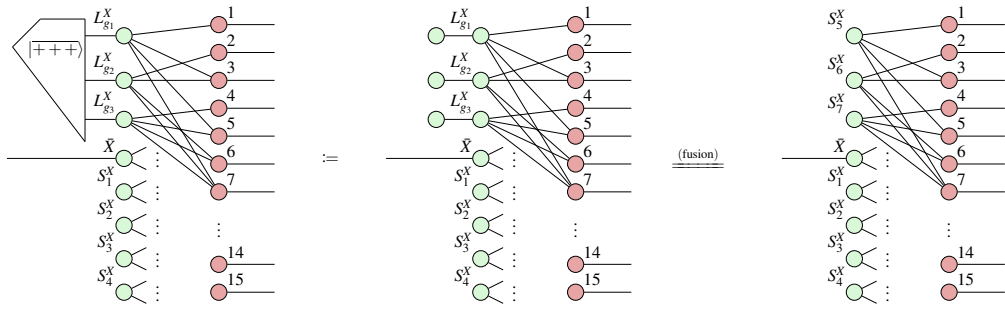
Figure 6:  $C_{sub}$  is equivalent to  $C_{ex}$  up to a fixed state of gauge qubits.

*Proof.* According to Def. 2.3, represent  $E_{sub}$  in the XZ normal form. With a sequence of rewrite rules, we obtain exactly the XZ normal form for  $E_{ex}$  which captures both the Z-type stabilizer generators  $S_i^z$

and the logical Z operators  $L_{g_j}^Z$ ,  $1 \leq i \leq 4$ ,  $1 \leq j \leq 3$ .



Alternatively, if one chooses to represent  $E_{sub}$  in the ZX normal form, the proof proceeds by applying the (fusion) rule to the Z spiders and identifying the gauge operators  $L_{g_1}^X$ ,  $L_{g_2}^X$ ,  $L_{g_3}^X$  of  $C_{sub}$  as the stabilizers  $S_5^X$ ,  $S_6^X$ ,  $S_7^X$  of  $C_{ex}$ , respectively:



□

**Corollary 5.1.** When the three gauge qubits are in the  $|\overline{000}\rangle$  state,  $C_{sub}$  is equal to  $C_{qrm}$ .

In [2, 51], code switching is described as a *gauge fixing* process. Further afield, [64] provides a generic recipe to gauge-fix a CSS subsystem code. Here, we generalize Lem. 5.1 and describe how to gauge-fix  $C_{sub}$  to  $C_{ex}$  using the ZX calculus.

**Proposition 5.2.** Gauge-fixing  $C_{sub}$  in the following steps results in  $C_{ex}$ , as shown in Fig. 7.

- (a) Measure three X-type gauge operators  $L_{g_i}^X$  and obtain the corresponding outcomes  $k_1, k_2, k_3 \in \mathbb{Z}_2$ .
- (b) When  $k_i = 1$ , the gauge qubit  $i$  has collapsed to the wrong state  $|\overline{-}\rangle$ . Apply the Z-type recovery operation  $L_{g_i}^Z$ .

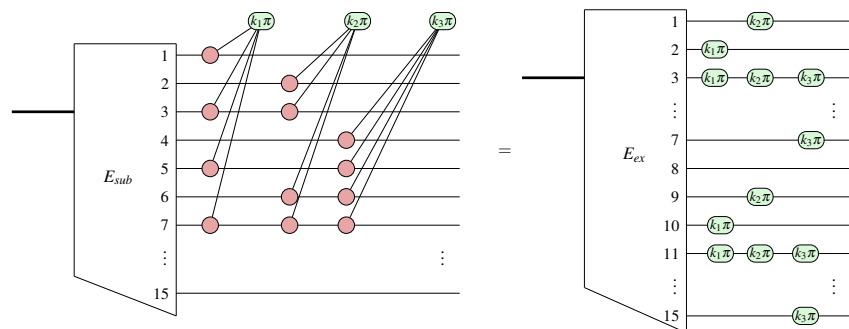
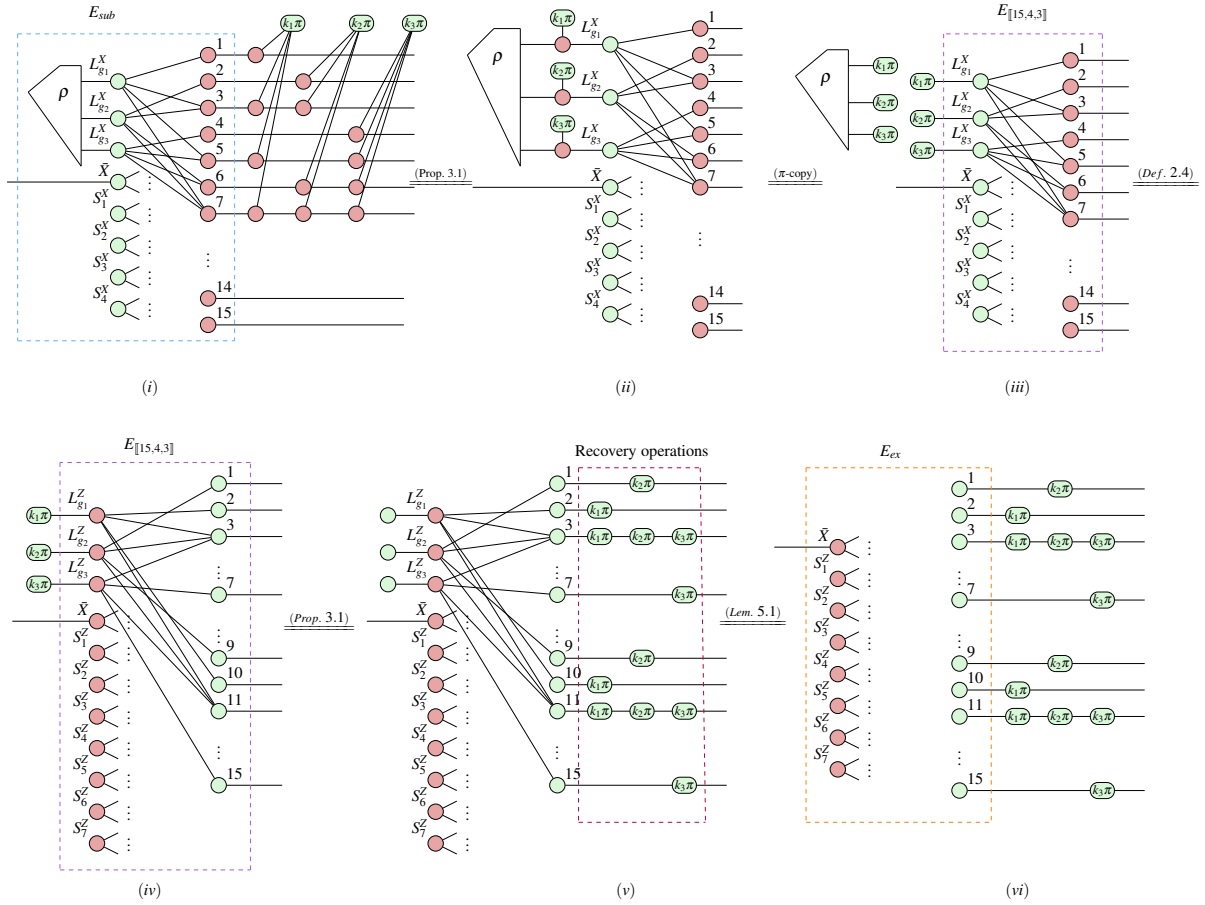


Figure 7: Gauge-fixing  $C_{sub}$  to  $C_{ex}$  in the circuit diagram.

*Proof.* By Def. 3.1, construct the ZX normal form of  $E_{sub}$  in the blue dashed box of (i). Then the three gauge operators  $L_{g_i}^X$  are measured in step (a). The subsequent equalities follow from Figs. 2 and 3. Next, we observe that the purple dashed box in (iii) is exactly the encoder of the  $[[15,4,3]]$  stabilizer code. By Lemma 3.2 in [39], it can be equivalently expressed in the XZ normal form, as in (iv). By Prop. 3.1, pushing each Z spider with the phase  $k_i\pi$  across  $E_{[[15,4,3]]}$  results in (v). In step (b), Pauli Z operators are applied based upon the measurement outcome  $k_i$ , which corresponds to the recovery operations in the red dashed box of (v). After that, the gauge qubits of  $\mathcal{C}_{sub}$  are set to the  $|+++ \rangle$  state. By Lem. 5.1, we obtain the XZ normal form for  $E_{ex}$ , as shown in the orange dashed box of (vi). Therefore, the equation in Fig. 7 holds.  $\square$



We sum up by explaining how to obtain  $\mathcal{C}_{ex}$  and  $\mathcal{C}_{qrm}$  by gauge-fixing  $\mathcal{C}_{sub}$ . In Prop. 5.2, we showed that measuring the X-type gauge operators  $L_{g_i}^X$  followed by the Z-type recovery operations  $L_{g_i}^Z$  is equivalent to adding  $L_{g_i}^X$  to the stabilizer group  $\mathcal{S}_{sub}$ . This results in the formation of  $\mathcal{C}_{ex}$ . Analogously, measuring the Z-type gauge operators  $L_{g_i}^Z$  followed by the X-type recovery operations  $L_{g_i}^X$  is equivalent to adding  $L_{g_i}^Z$  to  $\mathcal{S}_{sub}$ . Thus, we obtain  $\mathcal{C}_{qrm}$ .

Alternatively, gauge-fixing  $\mathcal{C}_{sub}$  can be viewed as a way of switching between  $\mathcal{C}_{ex}$  and  $\mathcal{C}_{qrm}$  [2, 53]. As an example, in Fig. 8, we visualize the measurement of  $L_{g_1}^X := X_1X_3X_5X_7$  in order to switch from  $\mathcal{C}_{qrm}$  to  $\mathcal{C}_{ex}$ . The effect of measuring other X-type gauge operators can be reasoned analogously.

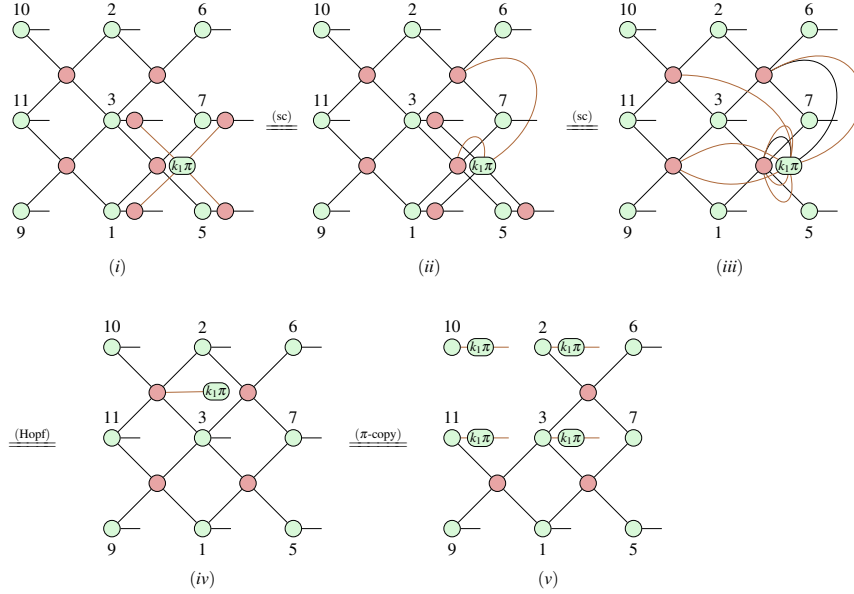


Figure 8: The switching from  $\mathcal{C}_{qrm}$  to  $\mathcal{C}_{ex}$  provides an alternative interpretation of Prop. 5.2. After measuring  $L_{g_1}^X$ ,  $L_{g_1}^Z$  is removed from the stabilizer group  $\mathcal{S}_{qrm}$  and the recovery operation is performed based on the measurement syndrome. Note that unrelated X and Z spiders are omitted from the ZX diagrams.

By Def. 3.1, construct the XZ normal form of  $E_{qrm}$  in (i). Then measure  $L_{g_1}^X$  and apply a sequence of rewrite rules to the ZX diagram. In (v), the stabilizer  $L_{g_1}^Z := Z_2Z_3Z_{10}Z_{11}$  is removed from the stabilizer group  $\mathcal{S}_{qrm}$ . Meanwhile, the recovery operation can be read off from the graphical derivation:  $(Z_2Z_3Z_{10}Z_{11})^{k_1} = (L_{g_1}^Z)^{k_1}$ ,  $k_1 \in \mathbb{Z}_2$ .

Overall, ZX visualization provides a deeper understanding of the gauge fixing and code switching protocols. On top of revealing the relations between different CSS codes' encoders, it provides a simple yet rigorous test for various fault-tolerant protocols. Beyond this, it will serve as an intuitive guiding principle for the implementation of various logical operations.

## 6 Conclusion

In this paper, we generalize the notions in [39] and describe a normal form for CSS subsystem codes. Built upon the equivalence between CSS codes and the phase-free ZX diagrams, we provide a bidirectional rewrite rule to establish a correspondence between a logical ZX diagram and its physical implementation. With these tools in place, we provide a graphical representation of two code transformation techniques: code morphing, a procedure that transforms a code through unfixing spiders for the stabilizer generators, and gauge fixing, where different stabilizer codes can be obtained from a common subsystem code. These explicit graphical derivations show how the ZX calculus and graphical encoder maps relate several equivalent perspectives on these code transforming operations, allowing potential utilities of ZX to simplify fault-tolerant protocols and verify their correctness.

Looking ahead, many questions remain. It is still not clear how to present the general code deformation of CSS codes using phase-free ZX diagrams. Besides, understanding code concatenation through the lens of ZX calculus may help derive new and better codes. In addition, it would be interesting to look at other code modification techniques derived from the classical coding theory [48].

## 7 Acknowledgement

The authors would like to thank Thomas Scruby for enlightening discussions. SML and MM wish to thank NTT Research for their financial and technical support. This work was supported in part by Canada's NSERC. Research at IQC is supported in part by the Government of Canada through Innovation, Science and Economic Development Canada. Research at Perimeter Institute is supported in part by the Government of Canada through the Department of Innovation, Science and Economic Development Canada and by the Province of Ontario through the Ministry of Colleges and Universities. LY is supported by an Oxford - Basil Reeve Graduate Scholarship at Oriel College with the Clarendon Fund.

## References

- [1] Scott Aaronson & Daniel Gottesman (2004): *Improved simulation of stabilizer circuits*. *Physical Review A* 70(5), p. 052328, doi:10.1103/PhysRevA.70.052328.
- [2] Jonas T Anderson, Guillaume Duclos-Cianci & David Poulin (2014): *Fault-tolerant conversion between the steane and reed-muller quantum codes*. *Physical Review Letters* 113(8), p. 080501, doi:10.1103/PhysRevLett.113.080501.
- [3] Frank Arute, Kunal Arya, Ryan Babbush, Dave Bacon, Joseph C Bardin, Rami Barends, Rupak Biswas, Sergio Boixo, Fernando GSL Brandao, David A Buell et al. (2019): *Quantum supremacy using a programmable superconducting processor*. *Nature* 574(7779), pp. 505–510, doi:10.1038/s41586-019-1666-5.
- [4] Miriam Backens (2014): *The ZX-calculus is complete for stabilizer quantum mechanics*. *New Journal of Physics* 16(9), p. 093021, doi:10.1088/1367-2630/16/9/093021.
- [5] H. Bombín & M. A. Martin-Delgado (2006): *Topological quantum distillation*. *Physical Review Letters* 97, p. 180501, doi:10.1103/PhysRevLett.97.180501.
- [6] H. Bombín & M. A. Martin-Delgado (2007): *Topological computation without braiding*. *Physical Review Letters* 98, p. 160502, doi:10.1103/PhysRevLett.98.160502.
- [7] Héctor Bombín (2015): *Gauge color codes: optimal transversal gates and gauge fixing in topological stabilizer codes*. *New Journal of Physics* 17(8), p. 083002, doi:10.1088/1367-2630/17/8/083002.
- [8] Robert I. Booth & Titouan Carette: *Complete ZX-calculi for the stabiliser fragment in odd prime dimensions*, doi:10.4230/LIPIcs.MFCS.2022.24. ISSN: 1868-8969.
- [9] A. R. Calderbank & Peter W. Shor (1996): *Good quantum error-correcting codes exist*. *Physical Review A* 54, pp. 1098–1105, doi:10.1103/PhysRevA.54.1098.
- [10] A Robert Calderbank, Eric M Rains, Peter W Shor & Neil JA Sloane (1997): *Quantum error correction and orthogonal geometry*. *Physical Review Letters* 78(3), p. 405, doi:10.1103/PhysRevLett.78.405.
- [11] Yudong Cao, Jhonathan Romero & Alán Aspuru-Guzik (2018): *Potential of quantum computing for drug discovery*. *IBM Journal of Research and Development* 62(6), pp. 6–1, doi:10.1147/JRD.2018.2888987.
- [12] Titouan Carette, Dominic Horsman & Simon Perdrix (2019): *SZX-calculus: scalable graphical quantum reasoning*. In: *44th International Symposium on Mathematical Foundations of Computer Science (MFCS 2019), Leibniz International Proceedings in Informatics (LIPIcs)* 138, Schloss Dagstuhl–Leibniz-Zentrum fuer Informatik, Dagstuhl, Germany, pp. 55:1–55:15, doi:10.4230/LIPIcs.MFCS.2019.55. Available at <http://drops.dagstuhl.de/opus/volltexte/2019/10999>.
- [13] Nicholas Chancellor, Aleks Kissinger, Joschka Roffe, Stefan Zohren & Dominic Horsman (2023): *Graphical Structures for Design and Verification of Quantum Error Correction*, doi:10.48550/arXiv.1611.08012. arXiv:1611.08012.
- [14] Julien Coudi (2022): *Cutting-edge graphical stabiliser decompositions for classical simulation of quantum circuits*. Master's thesis, University of Oxford.



- [15] Bob Coecke & Ross Duncan (2008): *Interacting quantum observables*. In: *ICALP, Lecture Notes in Computer Science*, pp. 298–310, doi:10.1007/978-3-540-70583-3\_25.
- [16] Bob Coecke & Ross Duncan (2011): *Interacting quantum observables: categorical algebra and diagrammatics*. *New Journal of Physics* 13(4), p. 043016, doi:10.1088/1367-2630/13/4/043016.
- [17] Bob Coecke & Aleks Kissinger (2017): *Picturing quantum processes*. Cambridge University Press, doi:10.1007/978-3-319-91376-6\_6.
- [18] Bob Coecke & Quanlong Wang (2018): *ZX-rules for 2-qubit Clifford+T quantum circuits*. In Jarkko Kari & Irek Ulidowski, editors: *Reversible Computation*, Springer International Publishing, Cham, pp. 144–161, doi:10.1007/978-3-319-99498-7\_10.
- [19] Oliver Cole (2022): *Quantum circuit optimisation through stabiliser reduction of Pauli exponentials*. Ph.D. thesis, Master’s thesis, University of Oxford. Available at <https://www.cs.ox.ac.uk/people/aleks.kissinger/theses/cole-thesis.pdf>.
- [20] Cole Comfort (2023): *The algebra for stabilizer codes*, doi:10.48550/arXiv.2304.10584. arXiv:2304.10584.
- [21] Alexander Cowtan (2022): *Qudit lattice surgery*, doi:10.48550/arXiv.2204.13228. arXiv:2204.13228.
- [22] Alexander Cowtan & Simon Burton (2023): *CSS code surgery as a universal construction*. arXiv preprint arXiv:2301.13738, doi:10.48550/arXiv.2301.13738.
- [23] Ross Duncan & Maxime Lucas (2014): *Verifying the Steane code with Quantomatic*. *Electronic Proceedings in Theoretical Computer Science* 171, pp. 33–49, doi:10.4204/eptcs.171.4. Available at <https://doi.org/10.4204/eptcs.171.4>.
- [24] Bryan Eastin & Emanuel Knill (2009): *Restrictions on transversal encoded quantum gate sets*. *Physical Review Letters* 102(11), p. 110502, doi:10.1103/PhysRevLett.102.110502.
- [25] Kun Fang, Jingtian Zhao, Xiufan Li, Yifei Li & Runyao Duan (2022): *Quantum NETWORK: from theory to practice*. arXiv preprint arXiv:2212.01226, doi:10.48550/arXiv.2212.01226.
- [26] Liam Garvie & Ross Duncan (2017): *Verifying the smallest interesting colour code with Quantomatic*. arXiv preprint arXiv:1706.02717, doi:10.4204/EPTCS.266.10.
- [27] Craig Gidney (2022): *A pair measurement surface code on pentagons*, doi:10.48550/arXiv.2206.12780. arXiv:2206.12780.
- [28] Craig Gidney & Austin G. Fowler (2019): *Efficient magic state factories with a catalyzed  $CCZ_i$  to  $2-T_i$  transformation*. *Quantum* 3, p. 135, doi:10.22331/q-2019-04-30-135.
- [29] Craig Gidney & Austin G. Fowler (2019): *Flexible layout of surface code computations using AutoCCZ states*, doi:10.48550/arXiv.1905.08916. Available at <https://arxiv.org/abs/1905.08916>.
- [30] Jonathan Gorard, Manojna Namuduri & Xerxes D. Arsiwalla (2021): *ZX-calculus and extended Wolfram model systems II: fast diagrammatic reasoning with an application to quantum circuit simplification*. arXiv preprint arXiv:2103.15820, doi:10.48550/arXiv.2103.15820.
- [31] D Gottesman (1999): *The Heisenberg representation of quantum computers*. In: *Group22: Proceedings of the XXII International Colloquium on Group Theoretical Methods in Physics*, pp. 32–43, doi:10.48550/arXiv.quant-ph/9807006.
- [32] Daniel Gottesman (1997): *Stabilizer codes and quantum error correction*. Ph.D. thesis, California Institute of Technology, doi:10.48550/arXiv.quant-ph/9705052.
- [33] Daniel Gottesman (1998): *Theory of fault-tolerant quantum computation*. *Physical Review A* 57, pp. 127–137, doi:10.1103/PhysRevA.57.127.
- [34] Daniel Gottesman (2022): *Opportunities and challenges in fault-tolerant quantum computation*. arXiv preprint arXiv:2210.15844, doi:10.48550/arXiv.2210.15844.
- [35] Amar Hadzihasanovic, Kang Feng Ng & Quanlong Wang (2018): *Two complete axiomatisations of pure-state qubit quantum computing*. In: *ACM/IEEE Symposium on Logic in Computer Science, LICS ’18*, Association for Computing Machinery, New York, NY, USA, p. 502–511, doi:10.1145/3209108.3209128.

- [36] Alexander Tianlin Hu & Andrey Boris Khesin (2022): *Improved graph formalism for quantum circuit simulation*. *Physical Review A* 105(2), doi:10.1103/physreva.105.022432.
- [37] Emmanuel Jeandel, Simon Perdrix & Renaud Vilmart (2020): *Completeness of the ZX-calculus*. *Logical Methods in Computer Science* Volume 16, Issue 2, doi:10.23638/LMCS-16(2:11)2020.
- [38] Andrey Boris Khesin, Jonathan Z. Lu & Peter W. Shor (2023): *Graphical quantum Clifford-encoder compilers from the ZX calculus*, doi:10.48550/arXiv.2301.02356. Available at <https://arxiv.org/abs/2301.02356>.
- [39] Aleks Kissinger (2022): *Phase-free ZX diagrams are CSS codes (... or how to graphically grok the surface code)*. *arXiv preprint arXiv:2204.14038*, doi:10.48550/arXiv.2204.14038.
- [40] Aleks Kissinger & John van de Wetering (2022): *Simulating quantum circuits with ZX-calculus reduced stabiliser decompositions*. *Quantum Science and Technology* 7(4), p. 044001, doi:10.1088/2058-9565/ac5d20.
- [41] Emanuel Knill & Raymond Laflamme (1997): *Theory of quantum error-correcting codes*. *Physical Review A* 55(2), p. 900, doi:10.1103/PhysRevLett.84.2525.
- [42] Emanuel Knill, Raymond Laflamme & Wojciech Zurek (1996): *Threshold accuracy for quantum computation*. *arXiv preprint quant-ph/9610011*, doi:10.48550/arXiv.quant-ph/9610011.
- [43] David Kribs, Raymond Laflamme & David Poulin (2005): *Unified and generalized approach to quantum error correction*. *Physical Review Letters* 94, p. 180501, doi:10.1103/PhysRevLett.94.180501.
- [44] Aleksander Kubica & Michael E. Beverland (2015): *Universal transversal gates with color codes - a simplified approach*. *Physical Review A* 91(3), p. 032330, doi:10.1103/PhysRevA.91.032330. arXiv:1410.0069.
- [45] Aleksander Kubica & Michael Vasmer (2022): *Single-shot quantum error correction with the three-dimensional subsystem toric code*. *Nature Communications* 13(1), p. 6272, doi:10.1038/s41467-022-33923-4.
- [46] Adrian Lehmann, Ben Caldwell & Robert Rand (2022): *VyZX: a vision for verifying the ZX calculus*. *arXiv preprint arXiv:2205.05781*, doi:10.48550/arXiv.2205.05781.
- [47] Sebastian Leontica, F Tennie & T Farrow (2021): *Simulating molecules on a cloud-based 5-qubit IBM-Q universal quantum computer*. *Communications Physics* 4(1), p. 112, doi:10.1038/s42005-021-00616-1.
- [48] F. J. MacWilliams & N. J. A. Sloane (1977): *The theory of error-correcting codes*. Elsevier.
- [49] Tommy McElvanney & Miriam Backens (2022): *Complete flow-preserving rewrite rules for MBQC patterns with Pauli measurements*, doi:10.48550/arXiv.2205.02009. arXiv:2205.02009.
- [50] Michael A. Nielsen & Isaac L. Chuang (2010): *Quantum computation and quantum information*, 10th anniversary ed edition. Cambridge University Press, doi:10.1017/CB09780511976667.
- [51] Adam Paetznic & Ben W. Reichardt (2013): *Universal fault-tolerant quantum computation with only transversal gates and error correction*. *Physical Review Letters* 111, p. 090505, doi:10.1103/PhysRevLett.111.090505.
- [52] David Poulin (2005): *Stabilizer formalism for operator quantum error correction*. *Physical Review Letters* 95(23), p. 230504, doi:10.1103/PhysRevLett.95.230504.
- [53] Dong-Xiao Quan, Li-Li Zhu, Chang-Xing Pei & Barry C Sanders (2018): *Fault-tolerant conversion between adjacent Reed–Muller quantum codes based on gauge fixing*. *Journal of Physics A: Mathematical and Theoretical* 51(11), p. 115305, doi:10.1088/1751-8121/aaad13.
- [54] Alexis T. E. Shaw, Michael J. Bremner, Alexandru Paler, Daniel Herr & Simon J. Devitt (2022): *Quantum computation on a 19-qubit wide 2d nearest neighbour qubit array*, doi:10.48550/arXiv.2212.01550. Available at <https://arxiv.org/abs/2212.01550>.
- [55] Peter W. Shor (1995): *Scheme for reducing decoherence in quantum computer memory*. *Physical Review A* 52, pp. R2493–R2496, doi:10.1103/PhysRevA.52.R2493.

- [56] Will Simmons (2021): *Relating measurement patterns to circuits via Pauli flow*. *Electronic Proceedings in Theoretical Computer Science* 343, pp. 50–101, doi:10.4204/eptcs.343.4.
- [57] Andrew Steane (1996): *Multiple-particle interference and quantum error correction*. *Proceedings of the Royal Society of London. Series A: Mathematical, Physical and Engineering Sciences* 452(1954), pp. 2551–2577, doi:10.1098/rspa.1996.0136.
- [58] Andrew M Steane (1996): *Simple quantum error-correcting codes*. *Physical Review A* 54(6), p. 4741, doi:10.1103/PhysRevA.54.4741.
- [59] Andrew M Steane (1999): *Quantum Reed-Muller codes*. *IEEE Transactions on Information Theory* 45(5), pp. 1701–1703, doi:10.1109/18.771249.
- [60] Felix Tennie & Tim Palmer (2022): *Quantum computers for weather and climate prediction: the good, the bad and the noisy*. *arXiv preprint arXiv:2210.17460*, doi:10.48550/arXiv.2210.17460.
- [61] Alex Townsend-Teague & Konstantinos Meichanetzidis (2022): *Classifying complexity with the ZX-calculus: Jones polynomials and Potts partition functions*. In: *Quantum Physics and Logic, Electronic Proceedings in Theoretical Computer Science (EPTCS 287)*, Oxford, p. 313–344. Available at [https://www.qplconference.org/proceedings2022/QPL\\_2022\\_paper\\_4.pdf](https://www.qplconference.org/proceedings2022/QPL_2022_paper_4.pdf).
- [62] Michael Vasmer & Aleksander Kubica (2022): *Morphing quantum codes*. *PRX Quantum* 3(3), doi:10.1103/prxquantum.3.030319.
- [63] Renaud Vilmart (2019): *A near-minimal axiomatisation of ZX-calculus for pure qubit quantum mechanics*. In: *LICS 2019*, pp. 1–10, doi:10.1109/LICS.2019.8785765.
- [64] Christophe Vuillot, Lingling Lao, Ben Criger, Carmen García Almudéver, Koen Bertels & Barbara M Terhal (2019): *Code deformation and lattice surgery are gauge fixing*. *New Journal of Physics* 21(3), p. 033028, doi:10.1088/1367-2630/ab0199.
- [65] Quanlong Wang (2018): *Qutrit ZX-calculus is complete for stabilizer quantum mechanics*. *Electronic Proceedings in Theoretical Computer Science* 266, pp. 58–70, doi:10.4204/EPTCS.266.3.
- [66] John van de Wetering (2020): *ZX-calculus for the working quantum computer scientist*. *arXiv preprint arXiv:2012.13966*, doi:10.48550/arXiv.2012.13966.
- [67] Theodore J. Yoder (2017): *Universal fault-tolerant quantum computation with Bacon-Shor codes*, doi:10.48550/arXiv.1705.01686. arXiv:1705.01686.
- [68] Qingling Zhu, Sirui Cao, Fusheng Chen, Ming-Cheng Chen, Xiawei Chen, Tung-Hsun Chung, Hui Deng, Yajie Du, Daojin Fan, Ming Gong et al. (2022): *Quantum computational advantage via 60-qubit 24-cycle random circuit sampling*. *Science bulletin* 67(3), pp. 240–245, doi:10.1016/j.scib.2021.10.017.